Electron-phonon heat transport in arrays of Al islands with submicrometer-sized tunnel junctions

J. P. Kauppinen and J. P. Pekola
Department of Physics, University of Jyväskylä, P.O. Box 35, 40351 Jyväskylä, Finland
(Received 13 June 1996)

We present experimental evidence of the effect of electrode volume and its shape on thermalization of small metallic islands for single electron tunneling. We have investigated the power law and the magnitude of the thermal transport and found that it obeys the common T^5 law for electron-phonon coupling only for the smallest islands studied, and in other cases considered, with cooling fins attached to the islands, the coupling per unit volume is weaker and it rather follows a law $\propto T^p$, where $p<5$. We attribute this to local hot electrons adjacent to the tunnel junctions. [S0163-1829(96)50736-8]

Thermalization of single-electron devices is of considerable current interest because of its fundamental and practical consequences. Heat transport between the conduction electrons and the lattice in a metal is believed to be well known and to obey a familiar $\propto T_e^5 - T_0^5$ law at low electron and lattice temperatures T_e and T_0, respectively. This law has been proven to be valid in thin films with uniform heating over a considerable surface area.[1–3] Preliminary investigations of this phenomenon in micrometer and submicrometer size samples exist, too.[4,5] Such structures are of intense interest because of their peculiar electrical transport properties. An important one of them is the well-known Coulomb blockade of tunneling in arrays of nanoscale junctions.[6,7] One of the main obstacles in investigation of such effects is the considerable thermal resistance limiting the minimum achievable temperature to some tens of millidegrees Kelvin. Our paper presents a fundamental experimental investigation of the thermalization of lithographically patterned tunnel junction arrays with thin-film micrometer-size metallic islands.

We fabricate our samples by electron-beam lithography and standard two-angle evaporation of aluminum with oxidation in between to create tunnel junctions with desired parameters. Measurements were carried out in a ^{3}He/^{4}He dilution refrigerator, and superconductivity of Al below 1 K was suppressed by magnetic field. Consider a linear array of N tunnel junctions connected together by normal-metal-island electrodes, shown by a scanning electron microscopy (SEM) micrograph in Fig. 1(a). When biased at a voltage V across the ends of the chain, we have a power generated in junction i which equals $V^2 R_{T,i}/R_T^2$ where $R_{T,i}$ is the resistance of the junction, typically 15–40 kΩ in this work, and $R_T = \Sigma_{i=1}^N R_{T,i}$. This power is evenly shared by the two neighboring islands. As will be shown below, this heat can hardly be transported away along the chain because of the high thermal resistance of the junctions, but it is, instead, leaking out from each island to the substrate via electron-phonon (el-ph) coupling and Kapitza resistance between the metal lattice and the silicon substrate, as depicted by the scheme in Fig. 1(b).

We base our analysis on the thermometric operation of arrays of normal-metal tunnel junctions in weak Coulomb blockade regime.[8,9] Assume an array perfectly thermalized at the (constant) temperature of the refrigerator at any bias voltage. In this case the shape of the differential conductance G closely follows the analytic form

$$G/G_T = 1 - (\epsilon_c/k_B T)\, g(eV/Nk_B T), \tag{1}$$

where G_T is the asymptotic conductance at high bias voltage, and the charging energy ϵ_c originates from the inverse-capacitance matrix of the array. Function g was introduced in Ref. 8: $g(x) = [x\sinh(x) - 4\sinh^2(x/2)]/[8\sinh^4(x/2)]$. If $\epsilon_c/k_B T \ll 1$, Eq. (1) is very well obeyed in experiment by any symmetric array if no thermal equilibrium problems appear. Suppose this is not true due to either an extremely low tem-

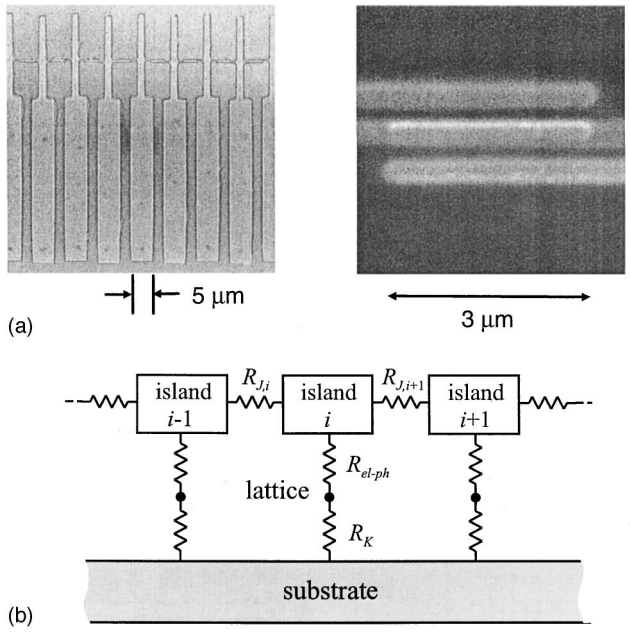

FIG. 1. (a) SEM micrographs of sections of a tunnel junction array used in this work. A section of a chain with extended islands on the left (type C as explained in the text), and a magnified view of one tunnel junction on the right. (b) A schematic thermal model of the array including the electronic thermal resistance of the junctions $R_{J,i}$, the el-ph resistance $R_{\text{el-ph}}$, and the Kapitza resistance to the substrate R_K.

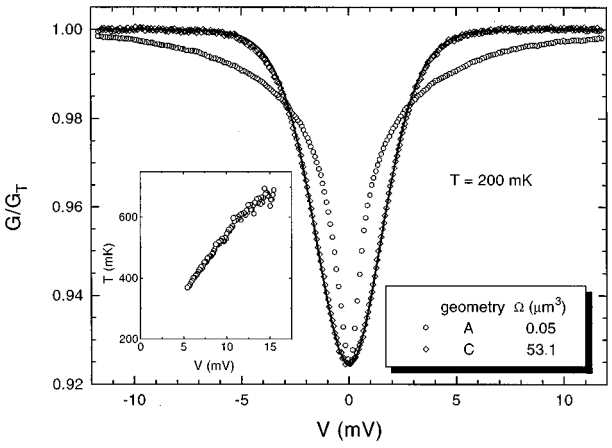

FIG. 2. Differential conductance G/G_T of two samples of types A and C at $T=200$ mK. The corresponding volumes Ω are indicated for each sample in the figure. The dependence with constant temperature [Eq. (1)] is shown by the solid line. The depth of the drop of the sample of type C has been scaled by 1.42, to allow direct comparison between the two samples and the constant temperature model. The inset shows the dependence of the electronic temperature of the small sample (type A) as plotted against bias voltage.

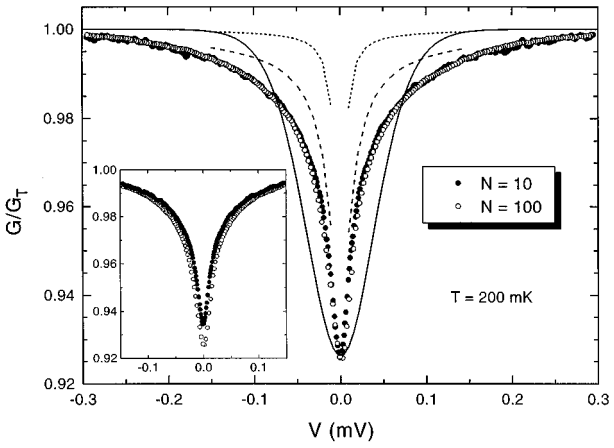

FIG. 3. Differential conductance G/G_T at $T=200$ mK of two samples which are similar except that the length of the array is $N=10$ in one case and $N=100$ in the other. The bias has been scaled by N to allow comparison [see Eq. (1)]. Also the heights of the peaks have been scaled to be equal. Peaks with unscaled heights are shown in the inset. The expected conductance curves assuming heat flux across the tunnel junctions, only, are shown by dashed and dotted lines for $N=10$ and 100, respectively. The solid line is the constant temperature prediction by Eq. (1).

perature and/or insufficient volume and surface area of the island electrodes to thermalize. In this case the electronic temperature increases upon increasing bias due to the power dissipated. The shape of the conductance curve is thus distorted from that of the nearly bell-shaped expression of Eq. (1).

This development is clearly demonstrated by our data in Fig. 2, where measured G/G_T curves for two samples with different island geometries are presented at a constant temperature of $T=200$ mK. The junctions in each case had a nominal overlap area of 0.25×3 μm^2 [Fig. 1(a)], and the island geometry for each set of data is indicated in the figure and its caption. We identify the sample geometries in the following as A, straight lines, 11×0.25 μm^2, connecting the junctions; B, an extension of 22×1.2 μm^2 added orthogonally to the geometry of A; C, an extension of 40×5 μm^2 further added to one end of the cooling fins of the geometry B. Data of samples of types A and C are shown in Fig. 2. Those of type B lie between these two extremes but these data have been omitted for clarity. The solid line represents the analytic form of Eq. (1) with the ϵ_c parameter chosen to fit the experimental depth. The data of the sample with increased volume of the island closely follow the constant-temperature curve but those of the array with small islands strongly deviate from this. We take this deviation as a quantitative measure of the thermal contact of the electrons on the islands to their surrounding lattice. Temperatures $T_e(V)$ calculated using Eq. (1) of the sample type A in Fig. 2 are shown in the inset.

In what follows we will discuss in detail how the heat channels out from the islands. In Fig. 3 we see data taken simultaneously of two different samples of type A on the same oxidized silicon substrate; the two arrays were otherwise similar (17 nm film thickness) but one of them was $N=10$ junctions long whereas the other one had $N=100$. The two curves, whose widths have been scaled by N, look practically identical and both of them strongly deviate from the constant temperature expression of Eq. (1), as indicated by the theoretical solid line. Suppose heat is predominantly carried away along the array. In this case the electronic thermal resistance of each junction introduces a temperature profile, with each island at its own temperature T_e and with increasing T_e toward the center of the chain. Furthermore, the longer the array, the wider is the temperature distribution. What this means in practice is that the arrays with $N=10$ and 100, respectively, should not be scalable in the way we have done in Fig. 3. This simple argument proves that the heat drains out from each island directly to the substrate, which legitimates our discussion of arrays with equal temperature for each island.

The argument above can be put on a more firm theoretical basis. The electronic heat transport rate P_i (without bias voltage) across a metallic normal-insulator-normal tunnel junction between electrodes i and $i+1$ can be simply written by golden rule arguments as

$$P_i=(e^2R_{T,i})^{-1}\int_{-\infty}^{+\infty}dEE[f_i(E)-f_{i+1}(E)], \qquad (2)$$

where $f_i(E)$ denotes the Fermi distribution function of electrode i at temperature T_i. If we denote the temperature difference between the two electrodes by $\Delta T_i\equiv T_i-T_{i+1}$, and assume it is small as compared to the two island temperatures considered, we arrive at an expression for the electronic thermal resistance of a tunnel junction as

$$R_{J,i}\equiv\Delta T_i/P_i=\frac{3e^2R_{T,i}}{\pi^2k_B^2T}. \qquad (3)$$

This represents a thermal resistance higher than any other resistance involved. We have numerically calculated the conductance curve assuming such thermal transport along the

array, only, for $N=10$ and 100 and the corresponding results are shown in Fig. 3 by a dashed and a dotted line, respectively.

The parallel thermal conductance has now been ruled out. We can also show that the bulk thermal resistances in series with the el-ph and the Kapitza boundary resistance do not contribute significantly. As a simple model, let us assume the island electrode embedded in the substrate material, which is silicon or fused silica. Thus, instead of an island on a planar surface we take, for simplicity, a spherical island with a radius r_0 giving approximately the same surface area as the actual planar-island electrode. For a spherically symmetric case, the temperature T_0 on the island producing heat at a rate P rises above that of the thermal bath at infinity, T_∞, as

$$T_0/T_\infty=\left(1+\frac{(b+1)P}{4\pi a r_0 T_\infty^{b+1}}\right)^{1/(b+1)}, \tag{4}$$

with the parameters a and b determining the thermal conductivity κ of the embedding material such that $\kappa=aT^b$. From Fig. 28 in Ref. 10, we obtain $a\simeq 6.4\ \mathrm{W\,m^{-1}\,K^{-3.68}}$ and $b\simeq 2.68$ in the range $1\leqslant T\leqslant 10$ K for silicon. Extrapolating this dependence to lower temperatures and inserting the numbers at $T_0=100$ mK, we obtain for $r_0=1\ \mu$m, a negligible temperature rise of $(T_0-T_\infty)/T_\infty\simeq 5\times 10^{-6}$ for a typical power level of $P=0.1$ pW. Thus, we may neglect the contribution of bulk thermal conductivity of the substrate; similarly we can rule out the effect of the Kapitza resistance between the bulk substrate and the sample holder by the argument of a large contact area in between. Thus, in summary, the observed thermal resistance is really from the island electrons to the substrate phonons.

By the argument of Wellstood, Urbina, and Clarke,[3] i.e., because the thin films cannot house phonons of short enough wavelengths at low temperature, we rule out the possibility that the Kapitza resistance would create a substantial temperature difference between the aluminum film and the bulk substrate. We thus conclude that the *main contribution to the nonequilibrium electronic temperature in excess of the base (refrigerator) temperature is caused by the finite electron-phonon coupling in the aluminum film.*

The el-ph coupling constant was extracted from the measured $G(V)/G_T$ in the following way. The charging energy ϵ_c of the array was first determined at high temperature (1–4 K) using the thermometric equilibrium shape of the conductance curve [Eq. (1)]. In fact,

$$\epsilon_c=\frac{6eV_{1/2}\Delta G/G_T}{5.439Nk_B}, \tag{5}$$

where $V_{1/2}$ and $\Delta G/G_T$ are the full width at half minimum and the depth of the conductance drop, respectively. Typically, values of ϵ_c/k_B range between 0.06 and 0.12 K for junctions with $\sim 0.8\ \mu\mathrm{m}^2$ area of this work.

At a lower temperature, where the shape of Eq. (1) is no longer followed due to the heating by the bias current, we analyzed the el-ph coupling at small temperature differences, i.e., near the minimum of the conductance dip. Assume first that the heating at zero bias is negligible, implying that $T_e=T_0$ at $V=0$; in other words, we apply a sufficiently small ac voltage to measure the differential conductance. Second, we assume that heating on each island equals V^2/NR_T. Third, the coupling between the electrons to the phonons is such that the power P of the heat transfer out of the electron system equals

$$P=\Sigma\Omega(T_e^n-T_0^n), \tag{6}$$

where Ω is the volume of the electrode, and Σ and n are the parameters of coupling. Literature gives $\Sigma\sim 1\ \mathrm{nW/K^5}\,\mu\mathrm{m}^3$ and $n=5$ for uniform heating in a metal.[1–4]

Using the three arguments above we may employ the following procedure to obtain Σ and n for a given sample. By Eq. (1) and the first argument, we obtain

$$T_0=\frac{(\epsilon_c/k_B)}{6\Delta G/G_T}, \tag{7}$$

where $\Delta G/G_T$ is the height of the dip. Next we fit the low bias range of the dip to a parabolic form

$$G/G_T=1-\Delta G/G_T(1-\alpha v^2) \tag{8}$$

with α as the fit parameter. Two typical examples of such fits are shown in Fig. 4(a). Here, $v\equiv eV/Nk_BT_0$. By a straightforward calculation one obtains

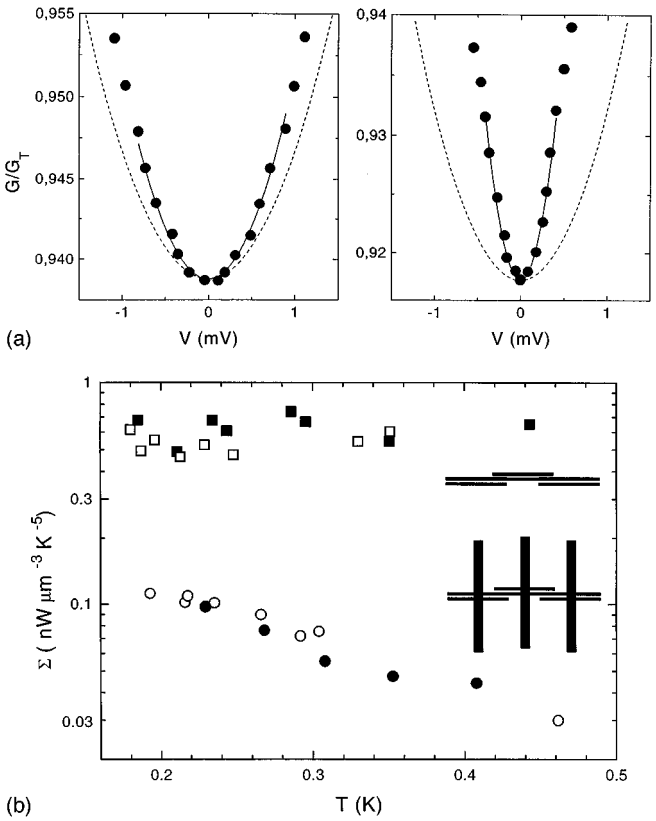

FIG. 4. (a) Typical examples of parabolic fits to the experimental conductance curves around zero bias to obtain the el-ph contact parameter. The sample on the left was of type B with $\alpha=0.161$, and the sample on the right was of type A with $\alpha=0.578$. (b) Thermal contact parameter Σ obtained for four different samples using the conventional $n=5$ power law. Squares, open and filled, are for nonextended islands of type A with film thicknesses 50 and 16 nm, respectively, whereas circles, open and filled, are for samples with extended islands of type B with film thickness of 13 nm in both cases.

$$\alpha = \frac{1}{10} + \frac{Nk_B^2}{n\Sigma\Omega R_T e^2 T_0^{n-2}}. \quad (9)$$

Thus a constant temperature (high T) dip has $\alpha = \frac{1}{10}$, where higher values of α at low temperature allow us to extract Σ for a given n.

In Fig. 4(b) we show a collection of data for four different samples of types A and B where a fit of $n=5$ has been applied to find Σ as a function of T_0. We note that for the nonextended samples of type A the el-ph coupling can be presented in the form $P=\Sigma\Omega(T_e^5-T_0^5)$, with $\Sigma \simeq 0.6$ nW/K$^5\mu$m^3. This applies for both thin (16 nm) and thicker (50 nm) films, indicating that increasing the thickness, and thus volume, improves the thermal contact.

For extended samples of type B, the contact is effectively weaker, and the dependence on T_0 is also weaker. The best fits in this case have $n \simeq 3.5$. Type C samples closely follow Eq. (1), and thus do not allow us to extract Σ.

The result of samples of type A agrees with the common expectation qualitatively and quantitatively. We are, however, unable to give a quantitative interpretation of the observation on the extended samples. Yet qualitatively it is obvious that, unlike in the majority of the earlier el-ph experiments,[1–3] heating in our case is local in the vicinity of the tunnel junctions. The observed temperature dependence with weaker power law is most likely due to the temperature dependence of the scattering lengths involved.[3]

In summary, we have been able to directly investigate the hot-electron effects in tunnel-junction arrays, which are of current interest for their Coulomb-blockade effects. At sufficiently low temperatures (<0.5 K) with sufficiently small straight islands, the thermalization is governed by the el-ph coupling with the familiar fifth-power difference in electronic and lattice temperatures, where the coupling parameter is $\Sigma = 0.6$ nW K$^{-5}\mu$m^{-3} for our Al samples. The thermal coupling can be improved by increasing the volume of the island, but, upon increasing the surface area alone, the effective coupling constant is reduced indicating the presence of local hot electrons.

We thank the Academy of Finland for financial support, and K. Chao, H. Müller, U. Heinke, K. Hirvi, A. Manninen, M. Manninen, M. Paalanen, P. Davidsson, and A. Korotkov for discussions.

[1] M. L. Roukes, M. R. Freeman, R. S. Germain, R. C. Richardson, and M. B. Ketchen, Phys. Rev. Lett. **55**, 422 (1985)

[2] F. C. Wellstood, C. Urbina, and J. Clarke, Appl. Phys. Lett. **54**, 2599 (1989)

[3] F. C. Wellstood, C. Urbina, and J. Clarke, Phys. Rev. B **49**, 5942 (1994)

[4] R. L. Kautz, G. Zimmerli, and J. M. Martinis, J. Appl. Phys. **73**, 2386 (1993)

[5] A. N. Korotkov, M. R. Samuelsen, and S. A. Vasenko, J. Appl. Phys. **76**, 3623 (1994)

[6] For reviews on the subject see, e.g., D. V. Averin and K. K. Likharev, in *Mesoscopic Phenomena in Solids*, edited by B. L. Altshuler, P. A. Lee, and R. A. Webb (Elsevier, Amsterdam, 1991), p. 173.

[7] *Single Charge Tunneling, Coulomb Blockade Phenomena in Nanostructures*, edited by H. Grabert and M. H. Devoret (Plenum, New York, 1992).

[8] J. P. Pekola, K. P. Hirvi, J. P. Kauppinen, and M. A. Paalanen, Phys. Rev. Lett. **73**, 2903 (1994)

[9] K. P. Hirvi, J. P. Kauppinen, A. N. Korotkov, M. A. Paalanen, and J. P. Pekola, Appl. Phys. Lett. **67**, 2096 (1995)

[10] S. M. Sze, *Physics of Semiconductor Devices* (Wiley, Singapore, 1981).